

Gravitational wave recoil in Robinson-Trautman spacetimes

Rodrigo P. Macedo*

Instituto de Física, Universidade de São Paulo, C.P. 66318, 05315-970 São Paulo, SP, Brazil

Alberto Saa†

Departamento de Matemática Aplicada, Universidade Estadual de Campinas, C.P. 6065, 13083-859 Campinas, SP, Brazil

(Received 17 September 2008; published 20 November 2008)

We consider the gravitational recoil due to nonreflection-symmetric gravitational wave emission in the context of axisymmetric Robinson-Trautman spacetimes. We show that regular initial data evolve generically into a final configuration corresponding to a Schwarzschild black hole moving with constant speed. For the case of (reflection-)symmetric initial configurations, the mass of the remnant black hole and the total energy radiated away are completely determined by the initial data, allowing us to obtain analytical expressions for some recent numerical results that have appeared in the literature. Moreover, by using the Galerkin spectral method to analyze the nonlinear regime of the Robinson-Trautman equations, we show that the recoil velocity can be estimated with good accuracy from some asymmetry measures (namely the first odd moments) of the initial data. The extension for the nonaxisymmetric case and the implications of our results for realistic situations involving head-on collision of two black holes are also discussed.

DOI: [10.1103/PhysRevD.78.104025](https://doi.org/10.1103/PhysRevD.78.104025)

PACS numbers: 04.30.Db, 04.25.dg, 04.70.Bw

I. INTRODUCTION

The possibility that a body recoils while emitting gravitational radiation has been known for decades [1]. This problem has been considered in the literature by means of many approximated and semianalytical methods as, for instance, the particle approximation [2], post-Newtonian methods [3], and the close-limit approximation [4], leading to typical recoil velocities of few hundreds of km/s for some realistic cases. Such conclusions, however, have changed drastically due to some recent advances in numerical relativity [5]. In particular, recent numerical simulations [6] of the merging process of binary black holes indicate that asymmetrical gravitational wave emission can indeed induce the merger remnant to recoil with velocities up to several thousands of km/s. The physical nature and possible implications of such considerably higher gravitational recoil are now under intense investigation (see, for instance, [7]). The calculation of the recoil velocity as a function of the black holes' initial conditions is a particularly important hard task. Since the full nonlinear regime of Einstein equations is extremely intricate and costly to analyze, some approximated or “empirical” formulas relating the recoil velocity and the initial data have been proposed [8].

The Robinson-Trautman (RT) spacetime [9] is perhaps the simplest solution of general relativity which can be interpreted as an isolated gravitational radiating system and, hence, it is certainly pertinent to the study of the gravitational recoil effect. However, despite the many

strong mathematical results on the RT solutions available in the literature, only a few exact examples of RT spacetime are indeed known in explicit form (see, for references, [10]). It is known, nevertheless, that a regular initial data, corresponding typically to a compact body surrounded by gravitational waves, will evolve smoothly according to the RT equation into a final state corresponding to a remnant Schwarzschild black hole [11], which can be at rest or moving with constant speed. Our aim here is to go a step further in the characterization of such a final evolution state as a function of the initial conditions. Our results are motivated and checked by some numerical analysis. The Robinson-Trautman partial differential equation has been analyzed numerically in the recent literature [12], being particularly suitable to be numerically solved by means of spectral methods [13–15]. We will follow Oliveira and Damião Soares [14,15] and adopt the Galerkin method [16] for our analysis. However, as we will show, we will implement it in a different way that will allow us to get simpler equations and better accuracy.

The present paper has four sections and one appendix. In the next section, the main aspects of axisymmetric RT spacetimes are presented briefly. We show, in particular, how to read from the final state of the RT evolution the mass and speed of the remnant black hole. It is also shown that, as expected, for (reflection-)symmetric initial data there is no radiation recoil. In such a case, the mass of the remnant black hole and the total energy radiated away are completely determined by the initial data, allowing us to establish analytical expressions for the results about the total radiated energy obtained numerically in [14,15]. Section III is devoted to the study of generic axisymmetric initial data. We show that a typical RT evolution can lead to

*romacedo@fma.if.usp.br

†asaa@ime.unicamp.br

a gravitational recoil. A Galerkin projection method is used to calculate the final black hole speed. We show also how the final recoil velocity can be estimated with good accuracy from some asymmetry measures of the initial configuration, namely, the first odd moments of the initial data. In the last section, we discuss the physical interpretation of the typical initial data considered in this work, emphasizing their relation with the problem of frontal collision of two black holes. The extension of our results to the non-axisymmetric case is also commented in the last section. The appendix presents a direct proof of a mathematical result used in Sec. II, namely, that, for regular initial data, the final state of the RT evolution does correspond generically to a Schwarzschild black hole moving with constant speed.

II. AXISYMMETRIC RT SPACETIME

The standard form of the RT metric in the usual spherical radiation coordinates (u, r, θ, ϕ) reads [10]

$$ds^2 = -\left(K - 2\frac{m_0}{r} - r(\ln Q^2)_u\right)du^2 - 2dudr + \frac{r^2}{Q^2}d\Omega^2, \quad (1)$$

where $Q = Q(u, \theta, \phi)$ and m_0 is a constant mass parameter. $d\Omega^2$ and K stand for, respectively, the metric of the unit sphere and the Gaussian curvature of the surface corresponding to $r = 1$ and $u = u_0$ constant, which is given by

$$K = Q^2\left(1 + \frac{1}{2}\nabla_\Omega^2 \ln Q^2\right), \quad (2)$$

with ∇_Ω^2 corresponding to the Laplacian on the unit sphere. Vacuum Einstein's equations for the metric (1) implies the Robinson-Trautman nonlinear partial differential equation [10]

$$6m_0 \frac{\partial}{\partial u} \left(\frac{1}{Q^2}\right) = \nabla_\Omega^2 K. \quad (3)$$

In this paper, we will focus on axisymmetric spacetimes and hence we will assume hereafter that $Q = Q(u, \theta)$. By introducing $x = \cos\theta$, one has

$$K = Q^2 + Q \frac{\partial}{\partial x} [(1-x^2)Q_x] - (1-x^2)Q_x^2 \quad (4)$$

and

$$6m_0 \frac{\partial}{\partial u} \left(\frac{1}{Q^2}\right) = [(1-x^2)K_x]_x, \quad (5)$$

where

$$\begin{aligned} [(1-x^2)K_x]_x &= (1-x^2)^2(QQ_{xxxx} - Q_{xx}^2) \\ &\quad - 8(x-x^3)QQ_{xxx} - 4(1-3x^2)QQ_{xx}. \end{aligned} \quad (6)$$

Integrating (5) and assuming a regular Gaussian curvature

K , one has

$$\frac{d}{du} \int_{-1}^1 \frac{dx}{Q^2(u, x)} = 0, \quad (7)$$

implying that the quantity $q_0 = \int_{-1}^1 Q^{-2} dx$ is constant along the solutions of (5). Notice that, from (1), the regularity of the surface u and r constants precludes us of having $Q = 0$. The regularity of the Gaussian curvature K , on the other hand, requires $0 < Q < \infty$. We normalize our data in order to have $q_0 = 2$, implying that the area of the surface corresponding to r and u constants is always $4\pi r^2$ along the u evolution governed by (5).

Several classical results assure that, given a geometrically regular initial data $Q(0, x)$, the solution of (5) approaches asymptotically a stationary ($Q_u = 0$) regime. The stationary solutions of (5) are such that

$$(1-x^2)K_x = A = \text{constant}, \quad (8)$$

leading to

$$K = A \operatorname{arctanh} x + B, \quad (9)$$

where B is another constant. Regularity of K on the interval $[-1, 1]$ requires necessarily $A = 0$. On the other hand, Eq. (4) implies that the regular Q solutions for which K is constant are such that $Q_{xx} = 0$ (see the appendix for a direct proof). Therefore, the stationary solutions of (5) are always of the form $Q = a + bx$ with a and b constants. Nevertheless, our choice of $q_0 = 2$ yields $a^2 - b^2 = 1$. We choose in this work a parametrization such that $a = \cosh\alpha$ and $b = \sinh\alpha$.

Given a normalized regular initial data $Q(0, x)$, the asymptotic solution of (5) will be always of the form $Q(\infty, x) = \cosh\alpha + x \sinh\alpha$. The final configuration is, hence, completely characterized by the sole parameter α . In order to unveil its physical role, let us consider the Bondi's mass function [17]

$$M(u) = \frac{m_0}{2} \int_{-1}^1 \frac{dx}{Q^3(u, x)} \quad (10)$$

which has several desirable properties to define an ‘‘instantaneous’’ mass for the solutions of (5); see, for instance, [14]. In particular, we have that $M(u) \geq m_0$ for normalized initial data and, for $u \rightarrow \infty$, it reduces to

$$\begin{aligned} M(\infty) &= \frac{m_0}{2} \int_{-1}^1 \frac{dx}{(\cosh\alpha + x \sinh\alpha)^3} = m_0 \cosh\alpha \\ &= \frac{m_0}{\sqrt{1-v^2}}, \end{aligned} \quad (11)$$

where $v = \tanh\alpha$ can be interpreted as the final velocity along the z axis of the remnant black hole [17].

The Bondi's mass (10) corresponds to the temporal component of the Bondi's four-momentum, which for generic (nonaxisymmetric) RT solutions is given by [17]

$$P_a(u) = \frac{m_0}{4\pi} \int_{S^2} \frac{\eta^a}{Q^3(u, \theta, \phi)} dS, \quad (12)$$

where S^2 is the unit sphere spanned by the usual coordinates θ and ϕ and with area element dS , and $a = 0, 1, 2, 3$, with $\eta^0 = 1$ and η^i being the radial three-vector directed to the point (θ, ϕ) on the unit sphere. For axisymmetric configurations, the nonvanishing components of the Bondi's four-momentum are $P_0(u) = M(u)$ and

$$P_3(u) = \frac{m_0}{2} \int_{-1}^1 \frac{x}{Q^3(u, x)} dx, \quad (13)$$

which corresponds to the momentum carried by the solution along the z axis. For normalized initial data one has for $u \rightarrow \infty$

$$P_a(\infty) = \frac{m_0}{\sqrt{1-v^2}} (1, 0, 0, -v), \quad (14)$$

reinforcing the interpretation of v as the final velocity of the remnant black hole.

Notice that, for symmetric (even) initial data $Q(0, x)$, Eq. (6) implies that the solutions $Q(u, x)$ of (5) are necessarily even for $u \geq 0$, establishing that there is no gravitational recoil ($v = 0$) in this case. Such a behavior is, of course, in full agreement with the expectation that gravitation recoil should be due to nonreflection-symmetric gravitational wave emission. Therefore, for even situations, the constraint (7) determines completely the final evolution state.

A. Radiated energy: reflection-symmetric case

The fraction of the initial mass $M(0)$ radiated away along the u evolution governed by (5) can be calculated exactly for even configurations. Following [14], we define

$$\Delta = \frac{M(0) - M(\infty)}{M(0)}, \quad (15)$$

which clearly corresponds to the fraction of the initial mass lost due to gravitational wave emission. For even configurations, $v = 0$ and we have simply

$$\Delta = 1 - 2 \left(\int_{-1}^1 \frac{dx}{Q^3(0, x)} \right)^{-1}. \quad (16)$$

It can be shown that $0 \leq \Delta < 1$. As an explicit example of this exactly soluble case, let us consider the first even initial data considered in the papers [14,15], namely, the prolate spheroid corresponding to

$$Q^2(0, x) = Q_0^2(1 - \epsilon^2 x^2), \quad (17)$$

with $0 \leq \epsilon < 1$. The constraint $q_0 = 2$ implies that

$$Q_0^2 = \frac{1}{2\epsilon} \ln \left(\frac{1+\epsilon}{1-\epsilon} \right), \quad (18)$$

leading finally to

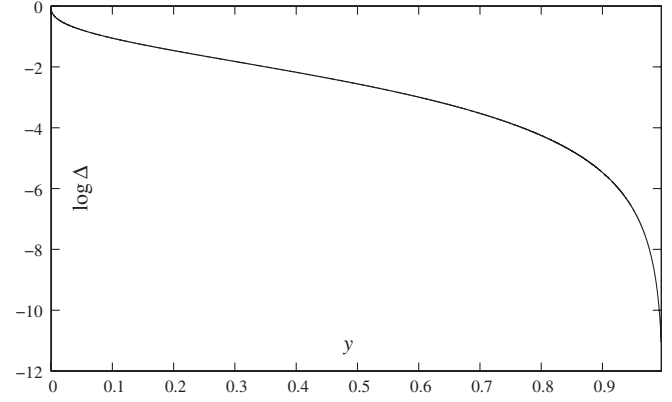


FIG. 1. The fraction Δ of the initial Bondi's mass lost due to gravitational wave emission for the initial configuration (17), as a function of $y = 1 - \epsilon$. The curve is in very good agreement with the one inferred from numerical results in [14,15]. Notice, however, that the nonextensive distribution function proposed in [14,15] is merely an approximation for $y \approx 1$; see (20).

$$\Delta = 1 - \sqrt{\frac{1-\epsilon^2}{8\epsilon^3} \ln^3 \left(\frac{1+\epsilon}{1-\epsilon} \right)}. \quad (19)$$

This is the exact analytical expression for the curves obtained in [14,15] from numerical simulations. For the sake of comparison with the results of [14,15], Fig. 1 depicts a semilog plot of Δ as a function of $y = 1 - \epsilon$, following their conventions. A very good agreement is found. One can proceed in an analogous way for any other even (reflection-symmetric) configuration, we will return to this issue in the last section. The exact expression for Δ is certainly valuable to the investigation of statistical properties of the nonlinear gravitational wave emission as those ones considered in [14,15]. For instance, it is clear from (19) that the nonextensive distribution function proposed in [14,15] is only an approximation valid for small ϵ . In fact, we have

$$\Delta = \frac{1}{30}(1-y)^4 + \frac{32}{945}(1-y)^6 + O((1-y)^8), \quad (20)$$

for $y \approx 1$ (or $\epsilon \approx 0$). Notice that $\Delta \rightarrow 1$ for $\epsilon \rightarrow 1$.

III. GENERAL SOLUTIONS

The evolution of generic initial data $Q(0, x)$ is a greater challenge. Since the gravitational recoil is clearly related to the odd part of the function $Q(u, x)$, one might consider in the first place some asymmetry measures of the initial data. The simplest ones correspond to their first odd n moments

$$q_n(u) = \int_{-1}^1 \frac{x^n}{Q^2(u, x)} dx, \quad (21)$$

which obey $-q_0 \leq q_n \leq q_0$. For the generic final evolution state $Q(\infty, x) = \cosh \alpha + x \sinh \alpha$, we have

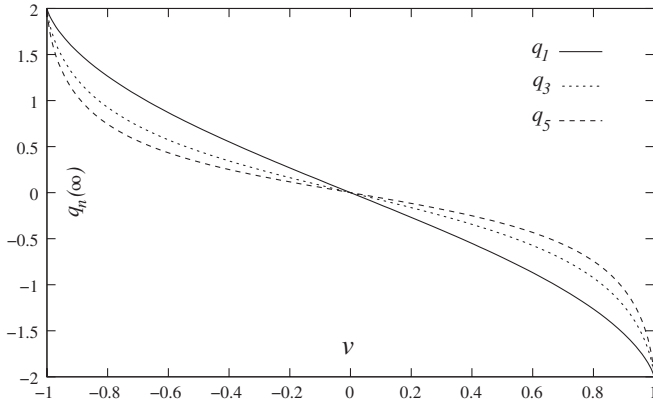


FIG. 2. Final odd moments $q_n(\infty)$, $n = 1, 3, 5$, as functions of the recoil velocity $v = \tanh\alpha$, as given by (22). Notice that, for a given $0 < |v| < 1$, one has $|q_1| > |q_3| > |q_5| > \dots$.

$$\begin{aligned} q_n(\infty) &= (1 - v^2) \int_{-1}^1 \frac{x^n}{(1 + vx)^2} dx \\ &= -\frac{1}{v^n} \left(2 - n \frac{1 - v^2}{v} \ln \frac{1 + v}{1 - v} \right) - \frac{1 - v^2}{v^{n+1}} \\ &\quad \times \sum_{k=2}^n \sum_{\text{odd } j} \frac{(-1)^k}{k-1} \binom{n}{k} \binom{k-1}{j} v^j, \end{aligned} \quad (22)$$

valid for odd n . Figure 2 shows the first final odd moments $q_n(\infty)$ as functions of the recoil velocity v . As we will show, the relevance of the first odd moments (21) rests on the fact that one can construct, as a linear combination of them, a second approximately conserved quantity along the solutions of the RT equation (5) in the framework of the Galerkin approximation.

A. The Galerkin method

We introduce now a Galerkin decomposition for $Q(u, x)$,

$$Q(u, x) = \sum_{\ell=0}^N b_\ell(u) P_\ell(x), \quad (23)$$

where $P_\ell(x)$ stands for the Legendre polynomials. By using standard projection techniques [16], Eq. (5) can be written as the system of ordinary differential equations

$$\dot{b}_\ell = -\frac{2\ell + 1}{24m_0} \langle Q^3[(1 - x^2)K_x]_v, P_\ell \rangle, \quad \ell = 0, 1, \dots, N, \quad (24)$$

where the inner product is given by $\langle f, g \rangle = \int_{-1}^1 f g dx$. From (6) and (23), one can see that the functions involved in the inner product in the right-hand side of (24) are simple polynomials in x . The integration can be performed exactly for arbitrary N (with the help of algebraic manipulation software as MAPLE, for instance), yielding 5th order polynomials on the mode functions b_ℓ . Notice that here, in contrast to the approach adopted in [14,15], no transcen-

dental function is involved in the Galerkin approximation. Now, the Cauchy problem for the RT equation corresponds basically to choose the initial value of the mode functions $b_\ell(u)$ according to

$$b_\ell(0) = \frac{2\ell + 1}{2} \langle Q(0, x), P_\ell \rangle, \quad (25)$$

and then to solve the initial value problem (IVP) given by (24).

Equation (24) has some useful properties that are independent of N . For instance, their stationary solutions ($\dot{b}_\ell = 0$) have necessarily $b_\ell = 0$ for $\ell > 1$ and arbitrary (constants) b_0 and b_1 . Indeed, for any regular initial data, the systems evolves into the final state $Q(\infty, x) = b_0(\infty)P_0(x) + b_1(\infty)P_1(x)$, with $b_0(\infty)^2 - b_1(\infty)^2 = 1$ for the normalized case, as expected. The recoil velocity will be given simply by $v = b_1(\infty)/b_0(\infty)$. Another useful property is that for an even initial data, one has $b_\ell(u) = 0$ for odd ℓ and, consequently, $v = 0$. The accuracy of the Galerkin decomposition is determined by the truncation order N in (23). It can be controlled effectively here by checking the conserved quantity q_0 along the u evolution. Typically, the expansion with N Legendre polynomials in (23) is accurate provided that $\max|b_N(u)|$ be small enough.

Finally, we are able now to consider the evolution of generic initial data. The recoil velocity v can be calculated by solving the IVP corresponding to the system of ordinary differential equations. (24) with initial conditions (25). The recoil velocity determines completely the final state for normalized initial data, allowing the study of any other relevant quantity as, for instance, the fraction Δ of the initial mass radiated away as a function of the nonreflection-symmetric initial data,

$$\Delta = 1 - \frac{2}{\sqrt{1 - v^2}} \left(\int_{-1}^1 \frac{dx}{Q^3(0, x)} \right)^{-1}. \quad (26)$$

We have performed an exhaustive numerical analysis of the system (24). The considered initial data include the following simple but representative family:

$$Q(0, x) = Q_0(1 + \alpha x + \beta x^2 + \gamma x^3), \quad (27)$$

where the constant Q_0 is always chosen in order to ensure the normalization $q_0 = 2$. Some particular elements of this family are presented in Fig. 3.

Figure 4 depicts a typical evolution for the modes $b_\ell(u)$ governed by (24) for a particular case of the family (27). The recoil velocity v can be read from the final state of the evolution for any initial data. We notice that, for the family of initial conditions (27), we always have $b_\ell(0) = 0$ for $\ell > 3$ and, in this case, $N = 8$ is sufficient to assure typically an accuracy (controlled by the constant $q_0(u) = 2$) of the Galerkin approximation up to 1%. Initial data with high $q_n(0)$ typically require higher N in order to attain a given accuracy. The radiation content of the initial data can

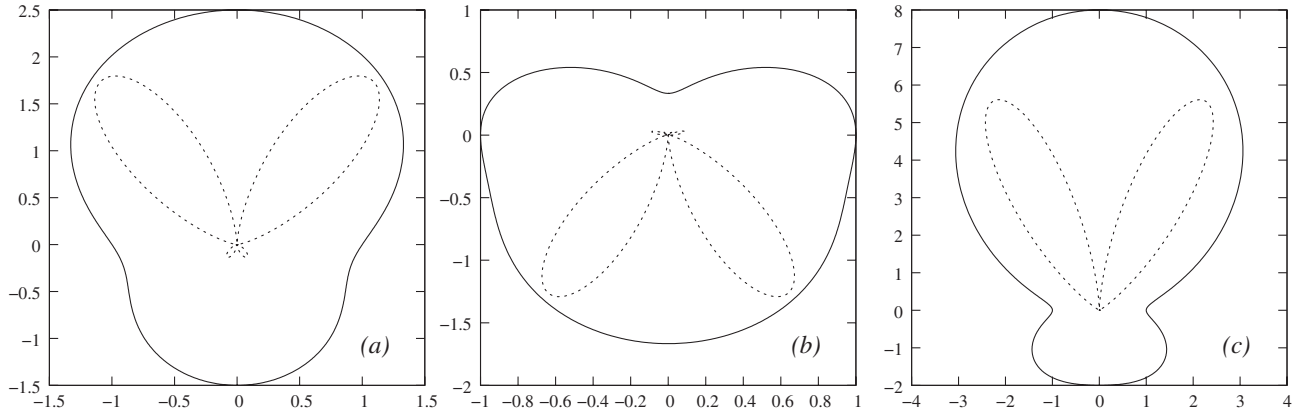


FIG. 3. Polar plot of some typical nonreflection-symmetric initial data $Q(0, x)$ of the family (27). The initial condition a , b , and c correspond, respectively, to the parameters $\alpha = 1/2$, $\beta = 1$, $\gamma = 0$; $\alpha = \beta = 0$, $\gamma = -2/3$; and $\alpha = 0$, $\beta = 4$, $\gamma = 3$. The dashed lines correspond to the associated gravitational radiation content (without scale); see Sec. IV.

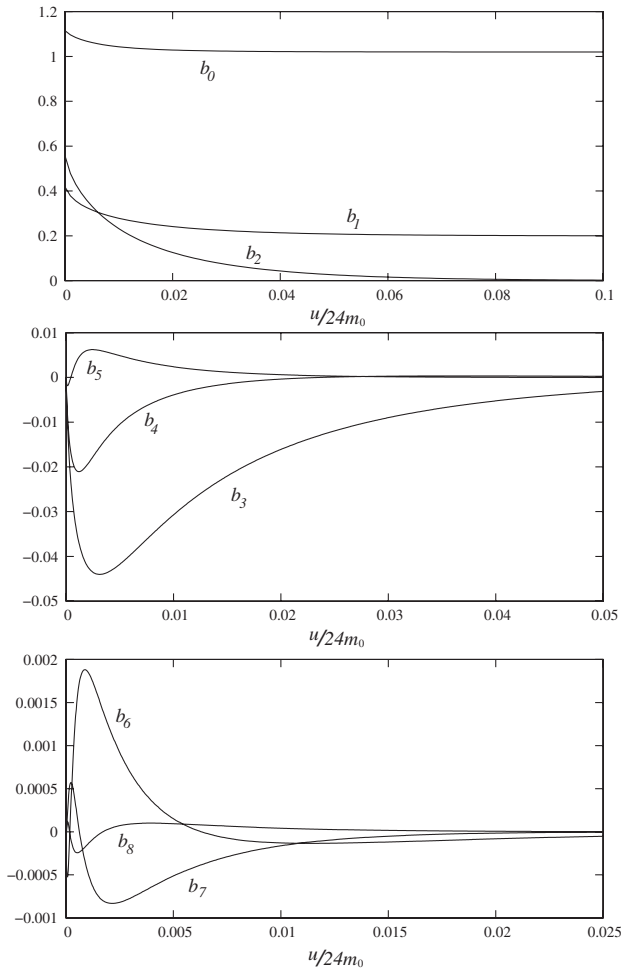


FIG. 4. Evolution of the modes $b_\ell(u)$ governed by (24) for the case (a) of Fig. 3. $N = 8$ was used, leading to an accuracy (controlled by the constant $q_0 = 2$) of 10^{-4} . The final evolution state has $b_0 = 1.0197$ and $b_1 = 0.20017$ and, consequently, the recoil velocity is $v = 0.19628$ and the radiated energy fraction $\Delta = 0.05420$, calculated according to (26).

also give some clues about the minimal necessary value of N ; see Sec. IV.

B. Estimation of the recoil velocity

Despite that the IVP associated to the Eq. (24) can be solved with quite modest computational resources, an analytical estimation of the recoil velocity v from the initial data would be certainly valuable. Since the final state of the RT evolution is completely characterized by the sole parameter v for normalized initial data, a second conserved quantity besides q_0 would suffice to determine completely the final state and, consequently, to determine the recoil velocity v . Unfortunately, the RT equation (5) does not seem to have any other conserved quantity rather than q_0 . On the other hand, its Galerkin approximation (24) does indeed have a second conserved quantity. Such a new conserved quantity, however, will be only approximately constant along the solutions of the full RT equation. Nevertheless, the approximation will be as good as the Galerkin approximation is accurate. In order to construct an explicit expression for the new constant, we remind you that (5) implies that the moments (21) obey the equation

$$6m_0\dot{q}_n(u) = \langle x^n, [(1-x^2)K_x]_x \rangle. \quad (28)$$

From (6) and (23), we see that

$$[(1-x^2)K_x]_x = \sum_{\ell=0}^{2N} a_\ell(u)x^\ell, \quad (29)$$

where $a_\ell(u)$ are quadratic functions of the modes $b_\ell(u)$. For odd n , the inner product in (28) will select only the odd- ℓ terms in x in the summation (29), leading to the following linear relation between $\dot{q}_n(u)$ and $a_\ell(u)$:

$$3m_0\dot{q}_n(u) = \sum_{\text{odd } \ell} \frac{a_\ell(u)}{\ell + n + 1}. \quad (30)$$

The right-hand side of (30) has exactly N terms, implying,

therefore, that one can have at most N linear independent equations of the type (28). The linear relation between \dot{q}_n and $a_\ell(u)$ given by (30) involves a Hilbert-type matrix [18] and, in particular, it is always possible to find $N + 1$ rational numbers α_ℓ such that

$$\frac{d}{du} \left(\sum_{\ell=1}^{N+1} \alpha_\ell q_{2\ell-1}(u) \right) = 0. \quad (31)$$

The quantity between parenthesis is conserved along the solutions of (24) and, therefore, it corresponds to our second conserved quantity. One could also truncate the summation in (30) in a given ℓ , obtaining a partial linear combination of the odd moments that are constant along the solutions of (24) up to deviations proportional to $\max |a_{\ell+2}(u)|$. The first of such partial linear combinations are

$$(\ell = 0) \quad q_1, \quad (32)$$

$$(\ell = 1) \quad q_1 - \frac{5}{3} q_3, \quad (33)$$

$$(\ell = 3) \quad q_1 - \frac{14}{3} q_3 + \frac{21}{5} q_5, \quad (34)$$

⋮

The coefficients in the above expressions and the α_ℓ of (31) can be calculated in a straightforward way by using, for instance, Gauss elimination in (30). However, our numerical calculations show that, for the typical initial data considered here, the first odd moment q_1 *dominates* over the other ones, implying that the typical variations $(q_1(0) - q_1(\infty))/q_1(0)$ are rather small. We notice also that the typical initial data of the family (27) considered here has $|q_1(0)| > |q_3(0)| > |q_5(0)| > \dots$, in agreement with the magnitude of the odd moments for the final state; see Fig. 2. This situation can fail for some very specific initial conditions. For instance, if one has $|q_3(0)| > |q_1(0)| > |q_5(0)| > \dots$, q_1 will vary considerably along the solutions of (24), but the combination given by (34) will be approximately constant, and so on. Figure 5 presents numerical evidences confirming these results. For practical purposes, whenever $|q_1(0)| > |q_3(0)| > |q_5(0)| > \dots$, one can assume that $q_1(\infty) \approx q_1(0)$ and estimate the final recoil velocity v as

$$\frac{1}{v} \left(2 - \frac{1-v^2}{v} \ln \frac{1+v}{1-v} \right) \approx - \int_{-1}^1 \frac{x}{Q^2(0,x)} dx. \quad (35)$$

In particular, v has the opposite sign of $q_1(0)$; see Fig. 5. We emphasize, nevertheless, that (35) will be accurate solely in the cases where $q_1(u)$ is actually the dominant moment.

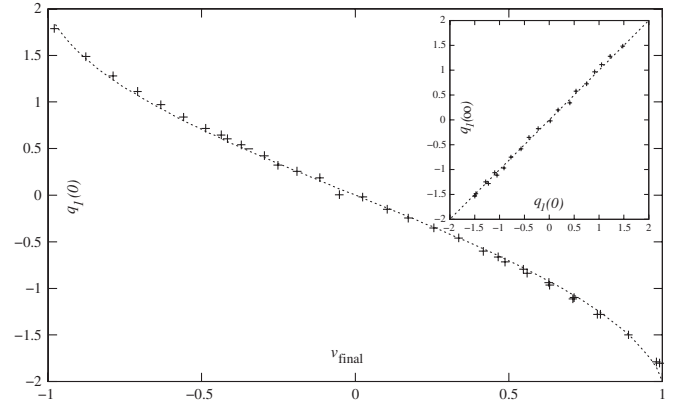


FIG. 5. Plot of $v \times q_1(0)$ for some typical regular initial conditions. The dotted line is the curve predicted by (35). The detail depicts the plot of $q_1(0) \times q_1(\infty)$. The assumption of $q_1(\infty) = q_1(0)$ is, typically, a good approximation when $q_1(u)$ is the dominant moment.

IV. DISCUSSION

The physical properties of the initial conditions corresponding to the family (27) can be investigated by considering their radiation content, which is determined by the $(1/r)$ -decaying part of the Riemann tensor and is proportional to the quantity [10,19]

$$D(u, x) = -(1 - x^2) Q^2 \partial_u \left(\frac{Q_{xx}}{Q} \right). \quad (36)$$

With the help of (5) and (6), one can show that for polynomials $Q(u, x)$ in x , the function $D(u, x)$ will be also polynomial in x . Moreover, $D(u, x)$ is an even (reflection-symmetric) function for even $Q(u, x)$. The dashed lines in Fig. 3 are polar plots without scale of $|D(0, x)|$ corresponding to the radiation content of the associated initial data. The asymmetry in the gravitational radiation emission responsible for the final recoil is clear. We notice that initial data with larger $\max |D(0, x)|$ will typically require a larger value of the truncation order N to attain a given accuracy in the Galerkin approximation. For instance, case (c) of Fig. 3 requires a truncation order larger than cases (b) and (a) to keep the same accuracy.

Some cases of the family (27) are especially interesting since they are good approximations for the Brill-Lindquist initial data [20]

$$Q(0, x) = Q_0 \left(\frac{1}{\sqrt{1-wx}} + \frac{\mu}{\sqrt{1+wx}} \right)^{-2}, \quad (37)$$

which can be interpreted as the final stage (after the horizon merging) of a frontal collision of two black holes [21,22], with the parameters $\mu \geq 0$ and $0 \leq w < 1$ related, respectively, to the mass ratio and to the infalling relative velocity of the two black holes. The constant Q_0 must be chosen in order to assure $q_0 = 2$. We have

$$Q_0^2(\mu, w) = \frac{1 + \mu^4}{1 - w^2} + \frac{4\mu(1 + \mu^2)}{\sqrt{1 - w^2}} + 3\frac{\mu^2}{w} \ln\left(\frac{1 + w}{1 - w}\right). \quad (38)$$

For $\mu = 1$ (the equal masses case), the function (37) is

$$\frac{1}{v} \left(2 - \frac{1 - v^2}{v} \ln \frac{1 + v}{1 - v} \right) \approx -q_1(0) = \frac{(\mu^{-2} - \mu^2) \left(\frac{1}{w^2} \ln \frac{1+w}{1-w} - \frac{2}{w-w^3} \right) + 8(\mu^{-1} - \mu) \left(\frac{\arcsin w}{w^2} - \frac{1}{w\sqrt{1-w^2}} \right)}{\frac{\mu^2 + \mu^{-2}}{1-w^2} + \frac{4(\mu + \mu^{-1})}{\sqrt{1-w^2}} + \frac{3}{w} \ln \left(\frac{1+w}{1-w} \right)}. \quad (39)$$

For small values of w , the condition (39) reduces to

$$v = \frac{\mu - 1}{\mu + 1} w. \quad (40)$$

Figure 6 shows the dependence of v with w for some values of μ as predicted by (39) and some numerical results. A very good agreement is found again. It is interesting to notice that

$$\lim_{w \rightarrow 1} q_1(0) = 2 \frac{\mu^4 - 1}{\mu^4 + 1} \quad (41)$$

for the initial data (37), implying from (39) that there exists a maximum recoil velocity for this configuration

$$\lim_{w \rightarrow 1} |v| = v_{\max} < 1. \quad (42)$$

In fact, Eq. (39) implies that $v < w$ for any μ (see Fig. 6), a behavior already noticed in the numerical analysis of [22]. One can also calculate the fraction (26) of the initial mass

reflection-symmetric and, in this case, the final state of the evolution is completely determined by the constraint $q_0 = 2$. For $\mu \neq 1$, one can estimate the recoil velocity for this head-on collision approximation by using (35). For the initial data (37) we have

radiated away for this case

$$\Delta = 1 - \frac{2}{\sqrt{1 - v^2}} \frac{Q_0^3(u, w)}{h(u, w)}, \quad (43)$$

where v is given by (39) and

$$h(u, w) = \frac{2(1 + \mu^6)}{(1 - w^2)^2} + \frac{8(\mu + \mu^5)}{(1 - w^2)^{3/2}} + \frac{15(u^2 + u^4)}{1 - w^2} + \frac{4(\mu + \mu^5) + 40\mu^3}{\sqrt{1 - w^2}} + \frac{15(\mu^2 + \mu^4)}{2w} \times \ln\left(\frac{1 + w}{1 - w}\right). \quad (44)$$

The aspect of the curves (43) are similar to that one depicted in Fig. 1. In particular, for small w , one has

$$\Delta = \frac{3}{5} \frac{\mu(5\mu^2 - 8\mu + 5)}{(\mu + 1)^4} w^4 + O(w^6), \quad (45)$$

compare with (20). Because of (42), one has $\Delta \rightarrow 0$ irrespective of μ for $w \rightarrow 1$.

We finish by commenting that the nonaxisymmetric case $Q = Q(u, \theta, \phi)$ can also be investigated by means of a Galerkin method. For such a case, the Galerkin decomposition (23) is based on the spherical harmonics

$$Q(u, \theta, \phi) = \sum_{\ell=0}^N \sum_{m=-\ell}^{\ell} b_{\ell m}(u) Y_{\ell}^m(\theta, \phi), \quad (46)$$

and a system of equations equivalent to (24) can be obtained. In this case, the stationary regime corresponds also to the case for that $b_{\ell m} = 0$ for $\ell > 1$. The constant- K final state will have the form

$$Q(\infty, \theta, \phi) = b_{00} + b_{10} \cos\theta + a \sin\theta \cos\phi + c \sin\theta \sin\phi, \quad (47)$$

where $b_{00}^2 - (b_{10}^2 + a^2 + c^2) = 1$ for the normalized case. The nonvanishing coefficients now can determine the modulus and the direction of the Bondi's four-momentum and, consequently, the recoil velocity of the remnant. These topics are now under investigation.

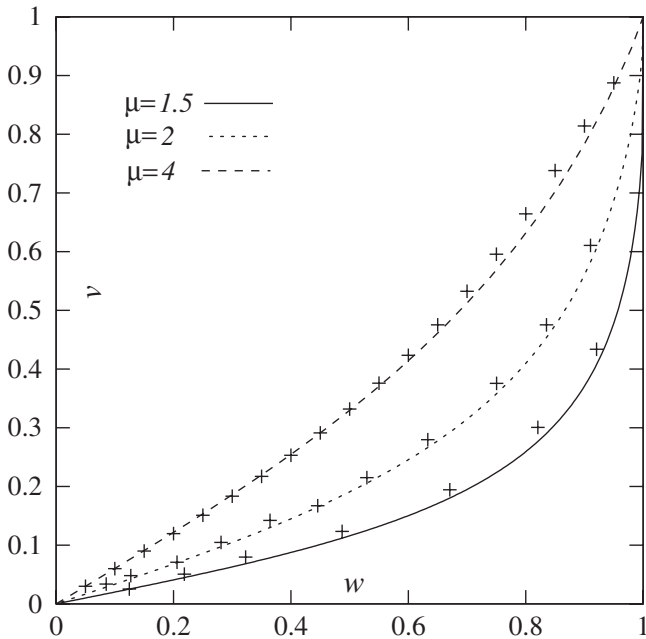


FIG. 6. Dependence of the recoil velocity v with the infalling velocity w of the two black holes with different masses, as predicted by (39), and some results from numerical calculations. Notice that $v \rightarrow -v$ if $\mu \rightarrow 1/\mu$.

ACKNOWLEDGMENTS

The authors are grateful to I. D. Soares, H. Oliveira, and R. Mosna for enlightening discussions. This work was supported by FAPESP and CNPq.

APPENDIX

One can check easily by a direct substitution that $Q(x) = a + bx$, with $a^2 - b^2 = K$, is a regular solution of (4). Nevertheless, a stronger result holds in this case: all regular solutions of (4) with constant K are necessarily of this form. We are interested in the geometrically regular solutions ($0 < Q(x) < \infty$ and $|Q_x(x)| < \infty$ for $-1 \leq x \leq 1$). The relevant phase space is three-dimensional and spanned by (x, Q, Q_x) . Notice that any solution such that $Q_{xx} = 0$ must be constrained on the surface \mathcal{L} of the phase

space corresponding to the points such that

$$L(x, Q, Q_x) = Q^2 - 2xQQ_x - (1 - x^2)Q_x^2 - K = 0. \quad (\text{A1})$$

One can show that, along any solution of (4), one has

$$(1 - x^2)Q \frac{dL}{dx} = 2(xQ + (1 - x^2)Q_x)L, \quad (\text{A2})$$

confirming that \mathcal{L} is indeed an invariant surface of (4). The linear equation (A2) has the solution

$$L(x, Q(x), Q_x(x)) = A \frac{Q^2(x)}{1 - x^2}, \quad (\text{A3})$$

where A is a constant, implying that any solution of (4) such that $L \neq 0$ cannot be regular in $x = \pm 1$.

-
- [1] W. B. Bonnor and M. A. Rotenberg, Proc. R. Soc. A **265**, 109 (1961); A. Peres, Phys. Rev. **128**, 2471 (1962); J. D. Bekenstein, Astrophys. J. **183**, 657 (1973).
- [2] M. J. Fitchett and S. Detweiler, Mon. Not. R. Astron. Soc. **211**, 933 (1984); T. Nakamura and M. P. Haugan, Astrophys. J. **269**, 292 (1983); M. Favata, S. A. Hughes, and D. E. Holz, Astrophys. J. **607**, L5 (2004); C. O. Lousto and R. H. Price, Phys. Rev. D **69**, 087503 (2004).
- [3] A. G. Wiseman, Phys. Rev. D **46**, 1517 (1992); L. E. Kidder, Phys. Rev. D **52**, 821 (1995); L. Blanchet, M. S. S. Qusailah, and C. M. Will, Astrophys. J. **635**, 508 (2005); T. Damour and A. Gopakumar, Phys. Rev. D **73**, 124006 (2006).
- [4] Z. Andrade and R. H. Price, Phys. Rev. D **56**, 6336 (1997); C. F. Sopuerta, N. Yunes, and P. Laguna, Phys. Rev. D **74**, 124010 (2006); **75**, 069903(E) (2007); Astrophys. J. **656**, L9 (2007).
- [5] F. Pretorius, Classical Quantum Gravity **22**, 425 (2005); Phys. Rev. Lett. **95**, 121101 (2005); M. Campanelli, C. O. Lousto, P. Marronetti, and Y. Zlochower, Phys. Rev. Lett. **96**, 111101 (2006); J. G. Baker, J. Centrella, D.-I. Choi, M. Koppitz, and J. van Meter, Phys. Rev. Lett. **96**, 111102 (2006).
- [6] J. A. Gonzalez, M. Hannam, U. Sperhake, B. Bruggmann, and S. Husa, Phys. Rev. Lett. **98**, 231101 (2007); M. Campanelli, C. O. Lousto, Y. Zlochower, and D. Merritt, Phys. Rev. Lett. **98**, 231102 (2007).
- [7] P. Madau and E. Quataert, Astrophys. J. **606**, L17 (2004); Z. Haiman, Astrophys. J. **613**, 36 (2004); A. Loeb, Phys. Rev. Lett. **99**, 041103 (2007); A. Gualandris and D. Merritt, Astrophys. J. **678**, 780 (2008); S. Komossa and D. Merritt, Astrophys. J. **683**, L21 (2008); L. Blecha and A. Loeb, arXiv:0805.1420.
- [8] K. S. Thorne, Rev. Mod. Phys. **52**, 299 (1980); L. E. Kidder, Phys. Rev. D **52**, 821 (1995); M. Campanelli, C. O. Lousto, Y. Zlochower, and D. Merritt, Astrophys. J. **659**, L5 (2007); C. O. Lousto and Y. Zlochower, Phys. Rev. D **77**, 044028 (2008); arXiv:gr-qc/0805.0159; S. H. Miller and R. A. Matzner, arXiv:0807.3028.
- [9] I. Robinson and A. Trautman, Phys. Rev. Lett. **4**, 431 (1960); Proc. R. Soc. A **265**, 463 (1962).
- [10] H. Stephani, D. Kramer, M. MacCallum, C. Hoenselaers, and E. Herlt, *Exact Solutions of Einstein's Field Equations* (Cambridge University Press, Cambridge, England, 2002), 2nd ed.
- [11] P. Chrusciel, Commun. Math. Phys. **137**, 289 (1991).
- [12] R. Gomez, L. Lehner, P. Papadopoulos, and J. Winicour, Classical Quantum Gravity **14**, 977 (1997); O. Moreschi, A. Perez, and L. Lehner, Phys. Rev. D **66**, 104017 (2002).
- [13] D. A. Prager and A. W.-C. Lun, Journal of the Australian Mathematical Society, Series B (Applied Mathematics) **41**, 271 (1999).
- [14] H. P. de Oliveira and I. Damião Soares, Phys. Rev. D **70**, 084041 (2004).
- [15] H. P. de Oliveira and I. Damião Soares, Phys. Rev. D **71**, 124034 (2005).
- [16] P. Holmes, J. L. Lumley, and G. Berkooz, *Turbulence, Coherent Structures, Dynamical Systems and Symmetry* (Cambridge University Press, Cambridge, England, 1998).
- [17] R. K. Sachs, Phys. Rev. **128**, 2851 (1962); H. Bondi, M. G. J. van der Berg, and A. W. K. Metzner, Proc. R. Soc. A **269**, 21 (1962); U. von der Goenna and D. Kramer, Classical Quantum Gravity **15**, 215 (1998).
- [18] M. D. Choi, Am. Math. Mon. **90**, 301 (1983).
- [19] H. P. de Oliveira, I. Damião Soares, and E. V. Tonini, Phys. Rev. D **78**, 044016 (2008).
- [20] D. R. Brill and R. W. Lindquist, Phys. Rev. **131**, 471 (1963).
- [21] O. M. Moreschi and S. Dain, Phys. Rev. D **53**, R1745 (1996).
- [22] R. F. Aranha, H. P. de Oliveira, I. Damião Soares, and E. V. Tonini, Int. J. Mod. Phys. D **17**, 55 (2008).